The International Journal of Advanced Manufacturing Technology (2023) 127:487–506
https://doi.org/10.1007/s00170-023-11506-x

ORIGINAL ARTICLE

Investigation of conventional and ANN-based feed rate scheduling methods in trochoidal milling with cutting force and acceleration constraints

Adam Jacso[1,2] · Tibor Szalay[1] · Basant Singh Sikarwar[2] · Rakesh Kumar Phanden[2] · Rajeev Kumar Singh[2] · Janakarajan Ramkumar[3]

Received: 28 December 2022 / Accepted: 29 April 2023 / Published online: 15 May 2023

Abstract
In CNC milling, the feed rate scheduling is a frequently used method to increase machining quality and efficiency. Among the benefits of feed rate scheduling, this paper focuses on controlling the tool load and optimizing the machining time. Although the advantages of feed rate scheduling are undeniable, some areas remain still to be addressed. In order to control the tool load, geometric methods are often used, which are based on keeping a specific parameter, such as chip thickness or material removal rate (MRR) constant. However, a high level of tool load control can only be provided if cutting force models or experimental-based techniques are used. Besides traditional methods, this paper presents an artificial neural network (ANN)-based feed rate scheduling method to keep the tool load constant, using data gained by preliminary cutting experiments. A case study demonstrates that a significantly higher level of tool load control can be achieved with this method as compared to the geometric models. Besides controlling the tool load, the present feed rate scheduling method also addresses the consideration of acceleration limits which is of great importance for practical uses. The application of feed rate scheduling in trochoidal milling is also discussed in detail in this paper. This area has not received enough attention, as due to the limited fluctuation of cutter engagement, the tool load was considered as well-controlled. However, experiments have shown that in the case of trochoidal milling, the introduction of feed rate scheduling can still further increase the machining efficiency. Using the developed ANN-based feed rate scheduling method, significant progress could be made as compared to conventional technologies in controlling the cutting force and optimizing the machining time. In the present case study, a reduction of 50% in machining time was achievable by adjusting the feed rate without increasing the peak value of cutting force.

Keywords Trochoidal milling · Feed rate scheduling · ANN · Cutter engagement · Cutting force · Acceleration constraints

1 Introduction

Metal cutting is still an important process in part manufacturing. In CNC milling, it is crucial to optimize the cutting parameters in order to provide maximum machining efficiency. Surface quality and accuracy are usually not critical for rough cutting operations. In these cases, the optimization criterion is typically the minimization of machining time, while the limitations are the provision of adequate tool life, the control of tool load, and the feasibility on the given machine tool [1]. The method presented in the paper also follows this approach. In many cases, using constant cutting parameters could not provide optimum performance. If the cutting conditions are changing along the tool path, adaptive feed rate must be used to increase the machining accuracy and productivity. By adjusting the feed rate, a nearly constant tool load can be provided which is essential for achieving short machining time, long tool life, and high machining accuracy.

Feed rate scheduling is a multi-purpose process. One of the most important goals is to increase machining accuracy.

✉ Adam Jacso
jacso.adam@gpk.bme.hu

[1] Department of Manufacturing Science and Engineering, Budapest University of Technology and Economics, Budapest, Hungary

[2] Department of Mechanical Engineering, Amity University, Noida, Uttar Pradesh, India

[3] Department of Mechanical Engineering, Indian Institute of Technology, Kanpur, Uttar Pradesh, India

By properly controlling the feed rate, the contour error can be significantly reduced [2, 3]. For smoothing the transition along corners, S-shape feed rate scheduling can be used [4]. To handle the accelerations and decelerations together, the bidirectional scanning technique is an effective method [5, 6]. Besides increasing the accuracy, another principal goal of feed rate scheduling is to reduce the machining time [7, 8]. This can be particularly effective if the curvature discontinuities are eliminated by local modification of the tool path along corners [9].

Increasing machining stability and safety is also a fundamental goal of feed rate scheduling. The variable cutting conditions caused by changing cutter engagement can be compensated with a properly adjusted feed rate [10]. There are two methods of tool load regulation in practice: online and offline monitoring and control. Online monitoring and control employ various sensors, while offline monitoring and control are simulation-based systems [11].

In case of online monitoring, it is possible to directly control the feed rate based on the measured cutting force [12, 13]. If tool load is monitored at check points only rather than continuously, and feed rate is adjusted accordingly, it offers economical solution as machining can be completed before tool life target [14]. However, usually the force measurement is only possible by using expensive and vulnerable sensors. In industrial applications, it is much easier to monitor the spindle current consumption [15].

The offline methods are usually more flexible and economical than the online monitoring and control systems [11]. Offline control of tool load requires the use of cutting force models [16, 17]. The cutting force is usually predicted using empirical formulas based on chip thickness and specific cutting force [18]. In recent years, in addition to geometric and mathematical models, neural network-based methods have also appeared [19, 20]. Maximum force constraints were used for rough machining, while maximum chip load constraints were used for semi-finishing and finishing in feed rate scheduling, and this attained 30% reduction in machining time [21]. The feed rate optimization based on cutting force prediction was introduced for finishing process of pocket milling. The cutting force prediction was based on model that included variation in feed direction, actual feed rate of metal cutting cross-section, and entry and exit angle of tool [22]. Machining time can be reduced by maximizing the cutting force to the acceptable level by a feed rate optimization strategy. Constraint-based optimization scheme combined with intelligent algorithm reduced the machining time by 26% experimentally than conventional NC part program [23]. A force-based model including new uncut chip thickness parameter showed the decrease in production time by 45–65% in feed rate optimization for ball end milling operation by keeping the cutting force under a preset threshold value [24]. An offline feed rate optimization for roughing process in CNC milling achieved 20% improvement in machining efficiency for casting/forging parts in experimental analysis [25]. Feed rate scheduling was achieved by the integration of mechanistic and geometric milling model for maintaining the cutting forces below maximum allowable limit in five axis-free form surface machining. This yielded a decrease in production time of blade machining by 35% [26].

However, the force models are not always available for feed rate scheduling, while determining them is costly and time-consuming. Therefore, various geometric methods have also been developed. Constant cutting forces were maintained through curvature-dependent feed rate with Pythagorean-hodograph curve fitting using CNC interpolators to achieve accuracy and longer tool life for varying MRR at a fixed depth of cut [27]. Although this method can be highly effective on low curvature tool path segments, the curvature-based feed control along sharp curves and corners is insufficient as the tool load begins to grow before the curvature starts to increase. This problem can be avoided by controlling the MRR. Feed rates were adaptively adjusted to maintain constant MRR using four different types of end mill cutters in 2.5D NC machining [28]. An octree-based NC simulation system was developed to work as offline adaptive control to optimize the feed rate in end milling operation [29]. Feed rate scheduling can also be based on keeping the chip thickness constant [30]. Although the geometric methods can be applied universally, it is not granted that keeping a cutting parameter such as MRR or chip thickness constant will result in a constant tool load.

Commercial software like VERICUT are the alternative to optimize the feed rate based on the cutting condition and ultimately improve surface finish and extend tool life [31]. Kurt et al. [32] systematically reviewed feed rate optimization techniques of CNC milling on sculptured surface using online and offline methods. This work was focused on capabilities of the present software packages, cutting force calculation methods, and MRR calculation approaches. Their study proved that commercial feed rate scheduling methods have some limitations because the MRR or the cutting force models are dependent on the given milling conditions.

Artificial intelligence methods can also be used to control the feed rate. A neural control adaptive strategy was used to maintain cutting force at a predetermined value to optimize feed rate in CNC milling process. This method showed good stability and high material removal rate [33]. For maintaining small variation in cutting force and maintaining constant roughness during CNC milling, a combination of neural networks, fuzzy logic, and particle swarm optimization (PSO) evolutionary strategy was used along with online adaptive controller. This solution was suitable for all geometry types, and adaptive controller was used for error compensation of optimization [34]. Feed rate optimization was demonstrated by ANN-based spindle power model by considering two

other constraints, viz., loading stability of spindle power and machining efficiency for three-axis rough milling [35].

The study of trochoidal machining has come to the forefront of research in the last two decades [36, 37] because this technology can ensure high productivity even when machining difficult-to-cut materials. Controlling the cutter engagement ensures stable machining conditions, which enables the use of high axial depth of cut, cutting speed, and feed rate without reducing tool life and the risk of tool breakage [38]. However, the application of feed rate scheduling in trochoidal milling has not received enough attention yet, as due to the limited fluctuation of cutter engagement, the tool load was be considered as well-controlled, and trochoidal milling typically requires a very high feed rate. However, for example, in the case of difficult-to-cut materials (such as superalloys), the feed rate usually remains far below the machine tool's capabilities [39], so significant reserves are available. Experiments have also shown that even in the case of trochoidal milling, the introduction of feed rate scheduling can still further increase the machining efficiency. An essential condition for feed rate scheduling is the control of tool load; otherwise, impermissible side effects could occur at extremely high cutting speeds and feed rates. García-Hernández et al. examined the traditional cycloidal tool path and achieved a 20% reduction in machining time by controlling the feed rate based on geometric methods [40]. There are advanced trochoidal tool path shapes where the fluctuation of cutter engagement are even smaller than in the case of conventional circular and cycloidal trajectories [41, 42]. Moreover, with the technique of constant engagement offsetting [43, 44], the cutting condition can be made completely uniform in the middle segment of the tool path [45]. However, feed rate scheduling is worth using even at these strategies, as the cutting conditions inevitably change during the rolling-in and out sections.

In this paper, the conventional geometric and regression-based methods and an ANN-based feed rate scheduling algorithm were experimentally and theoretically compared under straight and trochoidal milling conditions. The ANN-based feed rate scheduling method is proposed based on data retrieved from preliminary experiments. In contrast to the complex cutting force model, the proposed solution focuses only on the peak force of each tool rotation, as this is enough to control the tool load. This method provides better insight over tool load control in comparison to geometric models and also simplifies cutting force modelling. The presented feed rate scheduling method also takes into consideration the acceleration limits, which are necessary both for the precise machining time estimation and for ensuring an appropriate dynamic behaviour of the machine tool [46, 47]. The main innovation of the presented method is revealed in that the cutting force control and the consideration of acceleration limits are handled together in the ANN-based feed rate scheduling. Moreover, the presented experiments proved the suitability of the method in the case of trochoidal tool paths and also demonstrated its advantages compared to conventional approaches.

The framework of developed feed rate scheduling method is detailed in Section 2. The presented technique was experimentally verified for trochoidal milling, and it was found that saving in machining time up to 50 % is achievable by optimizing the feed rate. The experiments performed are discussed in Section 3. Finally, the results achieved and the opportunities for further development are summarized in Section 4.

2 The framework of developed feed rate scheduling method

In trochoidal milling, two aspects of feed rate scheduling have to be addressed: first is to control the cutting forces, and second is to consider the acceleration limits. In this section, the fulfilment of these criteria is described in detail.

2.1 Cutting force constraint

The offline feed rate scheduling solutions can be divided into two groups. The first type includes the geometrical methods, of which the chip thickness and the MRR based models have been examined. The other type includes the experimental methods based on preliminary measurements, of which the response surface methodology (RSM) and the ANN-based approaches have been investigated. Although this paper focuses on the ANN-based feed rate scheduling technique, the traditional geometrical approaches are also discussed because they were used as references when validating the developed feed rate scheduling method.

2.1.1 Geometrical methods

The most basic type of geometry-based feed rate scheduling methods is controlling the chip thickness. However, this can be accomplished in several ways since there are more approaches to interpreting the chip thickness. Because the shape of chip cross-section changes during the material removal process, deformed and undeformed (or uncut) chip thickness can be distinguished. Since the deformation process is extremely complex, the models used for feed rate adjustment are always based on undeformed chip thickness which has two types, namely, the maximum and average chip thickness. Both are possible bases for feed rate scheduling.

A simplistic 2D chip removal model of milling is shown in Fig. 1. To quantify the tool's radial immersion, the cutter engagement (θ) was used, which, in contrast to stepover (s) and radial depth of cut (a_e), accurately describes the

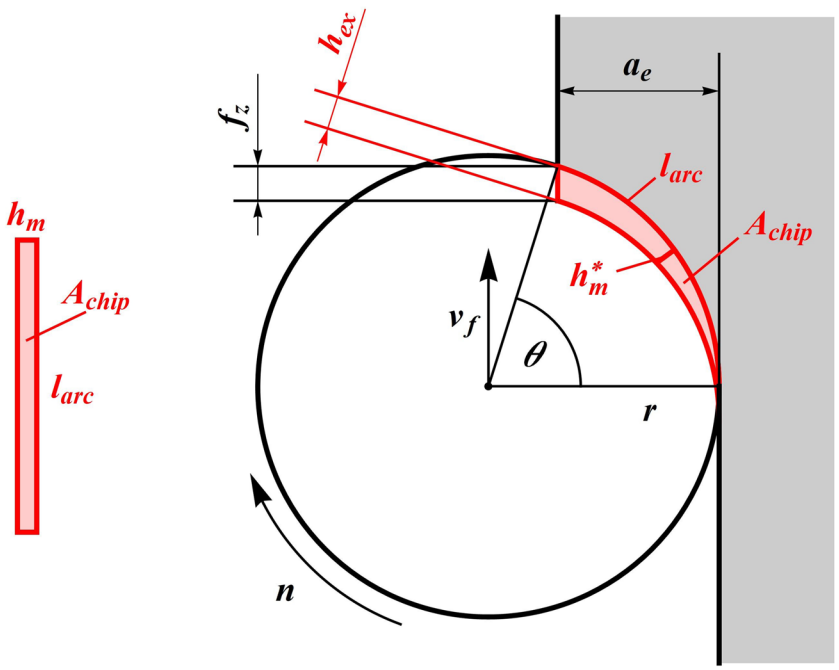

Fig. 1 The simplistic 2D chip removal model of milling (A_{chip}, chip cross-section; a_e, radial depth of cut; f_z, feed per tooth; h_{ex}, maximum chip thickness; h_m, h_m^*, average chip thickness; l_{arc}, chip's arc length; n, rotational speed; r, tool radius; v_f, feed rate; θ, cutter engagement)

interaction between the tool and the workpiece, even in the case of curved tool paths.

Several studies have been performed to describe chip thickness analytically. However, this paper only deals with the approach that considers the tool edge moves along a circular path instead of the real cycloidal trajectory. If the tool is not moving at an extremely high feed, the inaccuracy caused by this approximation is usually negligible in chip thickness [48]. Furthermore, the lead angle (κ) was considered 90°, as this is typical for tools used in trochoidal milling. Thus, the sinκ multiplier was not included in the formulas because it equals one.

Using the previous simplifications, the following approximation formula can be used to calculate the maximum chip thickness:

$$h_{ex}(\theta) = \begin{cases} f_z \sin\theta & if\, \theta \le 90° \\ f_z & if\, \theta > 90° \end{cases} [mm] \tag{1}$$

where $f_z\,[mm]$ is feed per tooth and $\theta\,[°]$ is cutter engagement angle.

The average chip thickness can be calculated by dividing the chip cross-section's area (A_{chip}) by the chip's arc length (l_{arc}) [49]. In this interpretation, the chip cross-section's area is equal to the product of radial depth of cut $(a_e\,[mm])$ and feed per tooth $(f_z\,[mm])$, and the chip's arc length is approximately equal to the product of tool radius ($r\,[mm]$) and central angle, i.e. the cutter engagement ($\theta\,[rad]$), in radian [50]. To simplify the formula, the relationship between radial depth of cut and cutter engagement can be used:

$$a_e(\theta) = r(1 - \cos\theta)\,[mm] \tag{2}$$

Based on these considerations, the average chip thickness can be derived as follows:

$$h_m(\theta) = \frac{A_{chip}}{l_{arc}} = \frac{a_e f_z}{r\theta} = \frac{(1-\cos\theta) f_z}{\theta}\,[mm] \tag{3}$$

It should be mentioned that the radial depth of cut (or stepover) is often used instead of the cutter engagement when defining the cutting parameters. Therefore, in industrial applications, another approximation formula is also common for calculating the average chip thickness [51]:

$$h_m^*(\theta) = f_z\sqrt{\frac{a_e}{d}}\,[mm] \tag{4}$$

where $d\,[mm]$ is the tool diameter. If Eq. (2) is applied to this formula, the expression can be simplified as follows:

$$h_m^*(\theta) = f_z\sqrt{\frac{1-\cos\theta}{2}}\,[mm] \tag{5}$$

Based on the previous formulas, it can be concluded that both the maximum and the average chip thickness can be expressed as a function of feed per tooth and cutter engagement. Figure 2 shows how the ratio of chip thickness to feed per tooth evolves as the cutter engagement changes. It can

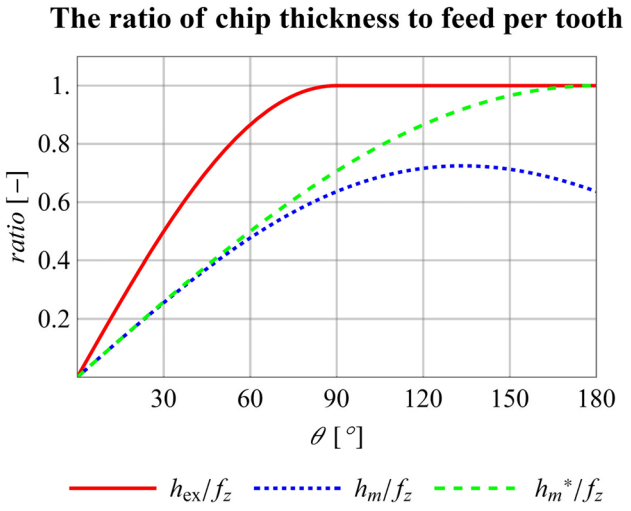

Fig. 2 The ratio of chip thickness to feed per tooth depending on cutter engagement

be noticed that the effect of cutter engagement differs significantly in the aspects of both maximum and average chip thickness. This fact predicts that the equivalent feed rates calculated by different geometric models will differ in the same way because (assuming a constant cutting speed) the feed rate $\left(v_f\right)$ is directly proportional to feed per tooth:

$$v_f = f_z\, zn\ \left[mm/min\right] \tag{6}$$

where $z\,[-]$ is the number of teeth and $n\left[rpm\right]$ is the spindle speed.

Thus, it is possible to determine how to adjust the feed rate as a function of cutter engagement to keep one of the chip thickness types uniform. Based on Eq. (1), the feed rate must be adjusted to keep the maximum chip thickness constant as follows (if both θ and θ_{ref} are less than or equal to 90°):

$$v_{f,h_{ex}}(\theta) = v_{f,ref}\frac{\sin\theta_{ref}}{\sin\theta}\ \left[mm/min\right] \tag{7}$$

where $v_{f,ref}\ \left[mm/min\right]$ is the appropriate feed rate for nominal cutter engagement $\theta_{ref}\,[°]$. It means that for a given cutter engagement θ, a feed rate of $v_{f,h_{ex}}(\theta)$ must be used to keep the maximum chip thickness at its original value, which is formed with the reference parameters $v_{f,ref}$ and θ_{ref}.

Based on Eq. (3) and Eq. (5), the equivalent feed rate to keep the average chip thickness constant can be calculated as follows:

$$v_{f,h_m}(\theta) = v_{f,ref}\frac{\left(1-\cos\theta_{ref}\right)\theta}{\left(1-\cos\theta\right)\theta_{ref}}\ \left[mm/min\right] \tag{8}$$

$$v_{f,h_m^*}(\theta) = v_{f,ref}\sqrt{\frac{\left(1-\cos\theta_{ref}\right)}{\left(1-\cos\theta\right)}}\ \left[mm/min\right] \tag{9}$$

Besides controlling the chip thickness, keeping the MRR is also a frequently used method in feed rate scheduling. This approach has become widespread primarily among the advanced cycles of CAM systems. MRR can be defined as the volume of material removed per unit time. There are two ways to interpret the value of MRR. Firstly, MRR can be calculated to the whole machining process, in which case it gives the productivity of machining. Secondly, the instantaneous value of MRR can also be interpreted, which expresses the magnitude of tool load. For feed rate scheduling, only the instantaneous MRR can be used, which can be describe with the following formula:

$$MRR(\theta) = a_p\, a_e\, v_f = a_p\, r(1-\cos\theta)\, v_f\ \left[mm^3/min\right] \tag{10}$$

where $a_p\,[mm]$ is axial depth of cut. Based on this formula, the equivalent feed rate to keep the MRR constant can be calculated as follows:

$$v_{f,MRR}(\theta) = v_{f,ref}\frac{1-\cos\left(\theta_{ref}\right)}{1-\cos\left(\theta\right)}\left[\frac{mm}{min}\right] \tag{11}$$

Compared to Eq. (8), the only difference between the two formulas providing constant average chip thickness or MRR is the θ/θ_{ref} multiplier. As this multiplication factor also increases with increase in the cutter engagement, the two feed rate scheduling methods will behave similarly relative to each other. Thus, compared to the constant MRR, a constant average chip thickness allows a higher feed rate at a cutter engagement greater than the nominal value and, conversely, a lower feed rate at a cutter engagement lower than the nominal value.

As shown in Fig. 3, the abovementioned methods lead to significantly different outcomes if the cutter engagement changes. The relationship between different geometric methods also depends on the nominal cutter engagement. If the cutter engagement is smaller than the nominal value, keeping the maximum chip thickness constant is the strictest condition, followed by controlling the average chip thickness, whichever approximation formula is used, and the highest equivalent feed rate is obtained by keeping the MRR constant. If the cutter engagement is larger than the nominal value, the opposite trends can be observed.

It can be noticed that the previous formulas for equivalent feed rate differ considerably from each other. In addition, keeping a geometric parameter constant does not mean that the tool load will remain constant. A further disadvantage of chip thickness-based methods is that the number of active tool edges can also vary as the cutter

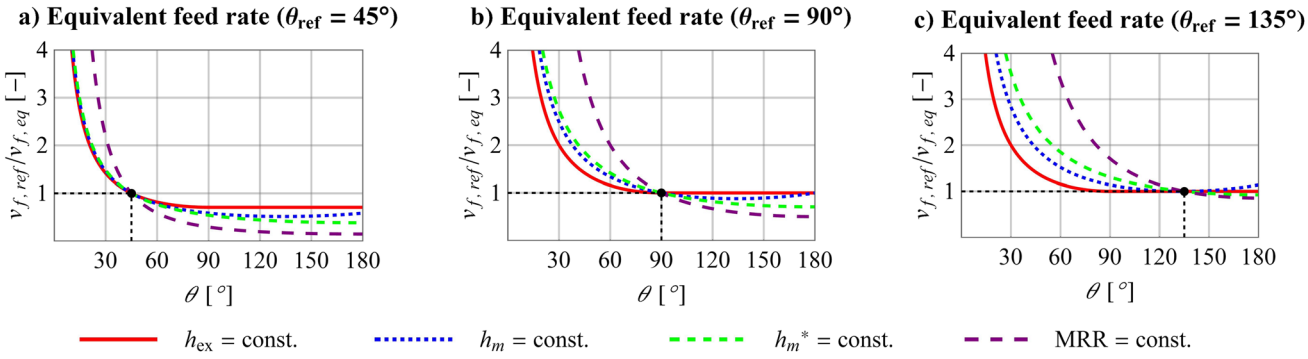

Fig. 3 The equivalent feed rate calculated by geometrical methods in case of different nominal cutter engagements

engagement changes, especially in the case of a high number of teeth and a large helix angle. This problem also exists if the MRR-based methods are used, albeit to a lesser extent. In addition, the effect of tool geometry cannot be considered by these methods either. Therefore, keeping the tool load constant is only possible based on experimental data.

2.1.2 Experimental methods with traditional regression models

A high-level solution for controlling the tool load can be applied if an accurate cutting force model is available to adjust the feed rate. This requires the knowledge of cutting force coefficients and the calculation of local chip thickness of varying magnitude along the tool edge. However, the drawback of this method is that the determination of cutting force coefficients is costly and time-consuming. Also, several external influencing factors such as tool wear, lubrication conditions, vibrations, and tool run-out can affect the model's accuracy [52].

Considering that an accurate cutting force model can be determined only experimentally, this paper recommends the direct use of data collected under specific conditions for controlling the feed rate. This approach also avoids double calculations that would be required if a force model were first created to recalculate the equivalent feed rate.

Although determining the optimal cutting parameters is a complex problem, it simplifies the issue that the axial depth of cut and the cutting speed can be considered constant in feed rate scheduling. Therefore, the purpose is to create a model that can determine the equivalent feed rate for a given cutter engagement at which the tool load is as high as with the nominal parameters. In other words, an approximation function $v_{f,eq}(F,\theta)$ must be determined, which can be applied with different tool load limits.

There are several ways to describe the function $v_{f,eq}(F,\theta)$ that provides a constant cutting force of magnitude F at any cutter engagement θ. In the field of RSM, the linear regression models are the most common. In this approach, the general form of a complete second-degree polynomial regression model in two variables can be described as follows:

$$v_{f,reg_{2nd}}(F,\theta) = c_0 + c_1F + c_2\theta + c_3F^2 + c_4\theta^2 + c_5F\theta \left[\frac{mm}{min}\right] \tag{12}$$

where c_i are constant coefficients. However, the case study presented in Sect. 3 will show that the second-order model cannot provide sufficient complexity. Therefore, the third-degree model is also examined in this paper, which can be described as follows:

$$\begin{aligned} v_{f,reg_{3rd}}(F,\theta) &= c_0 + c_1F + c_2\theta + c_3F^2 + c_4\theta^2 \\ &+ c_5F\theta + c_6F^3 + c_7\theta^3 + c_8F^2\theta + c_9F\theta^2 \left[\frac{mm}{min}\right] \end{aligned} \tag{13}$$

The exponential approximation formulas are also frequently used in the field of cutting force modelling. Thus, an exponent based model was also tested:

$$v_{f,reg_{exp}}(F,\theta) = c_0 + c_1F^{\alpha}\theta^{\beta} \left[\frac{mm}{min}\right] \tag{14}$$

where α and β are power exponents.

For these models, sample data are required to determine the constant parameters. If measurements are performed with different cutting parameters to generate experimental data, the constant parameters can be calculated using the method of least squares.

Although the developed ANN-based feed rate scheduling model is also based on preliminary experimental results, it will be covered in a separate subsection.

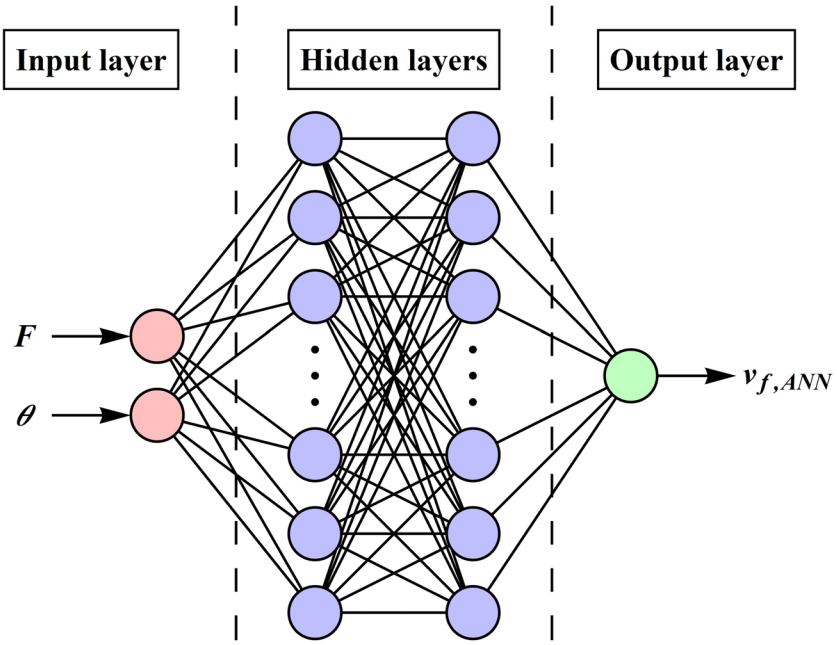

Fig. 4 The structure of ANN for calculating the equivalent feed rate

2.1.3 Experimental method with ANN

For modelling the equivalent feed rate, a multi-hidden layer neural network was implemented in the software Wolfram Mathematica 12 (refer to Fig. 4). The input layer had two neurons for the parameters F and θ, and the output layer had only one neuron for the equivalent feed rate $\left(v_{f,ANN}\right)$. According to the references mentioned in Sect. 1, two hidden layers were applied in the neural network. To determine the appropriate settings of the neural network, systematic tests were performed where the effects of the number of neurons (5–50), the type of activation function (rectified linear unit, logistic sigmoid, hyperbolic tangent), and the choice of optimization algorithm (Adam optimizer, root mean squared propagation, stochastic gradient descent) were examined. As a result of this analysis, 20 neurons per layer, the logistic sigmoid activation function and the Adam optimizer method were selected. Xie et al. obtained a similar result when modelling the spindle power as a function of cutting parameters [35]; however, they used few neurons (nine per layer). The training of neural network was performed by the built-in algorithms of Wolfram Mathematica. For training the neural network, the data set was randomly divided into training (80%) and validation (20%) sets. During the experiments, the problem of overfitting never occurred with the settings mentioned above.

As a practical example will demonstrate in Sections 3.3 and 3.4, the ANN-based modelling of equivalent feed rate can give a more accurate result than the conventional regression models. In addition, there is another advantage of this approach, namely, that the problem of choosing the appropriate regression formula does not have to be addressed. The neural network can adapt universally to any trend between the input data and the appropriate feed rate.

2.2 Acceleration constraints

Besides balancing the fluctuation of tool load, it is also important to consider the machine tool's acceleration capabilities. When analysing the accelerations, it is advisable to treat normal and tangential components separately. Both types of acceleration can be a limiting factor when calculating the feasible feed rate along the tool path considering the capabilities of a given machine tool. In fact, there is no detrimental effect on machining if a higher feed rate is programmed, as the CNC controller would limit the speed. However, without analysing the accelerations, the machining time estimation could be highly inaccurate, which could lead to an erroneous decision when optimizing the cutting parameters.

2.2.1 Centripetal acceleration

Besides the controlling of tool load, consideration of centripetal acceleration is the most severe constraint which can be expressed as follows:

$$a_c = \frac{{v_f}^2}{3600\,\rho}\left[mm/s^2\right] \tag{15}$$

where $\rho\,[mm]$ is the path curvature radius. Centripetal acceleration can be critical along corners and arcs with a small

curvature radius. In such cases, a reduction in feed rate is necessary to keep the centripetal acceleration within the machine tool's capabilities.

2.2.2 Tangential acceleration

The consideration of tangential acceleration is necessary if the path tracking speed is not constant. However, when controlling the feed rate, this is the case for most section of the path. The tangential acceleration can be described as follows:

$$a_t = \frac{\Delta v_f}{60\,\Delta t}\left[mm/s^2\right] \tag{16}$$

where $\Delta v_f\left[mm/min\right]$ is the change in feed rate over the time $\Delta t\,[s]$.

Tangential acceleration can act as a limiting factor for both accelerating and decelerating. Along the acceleration sections, it is easy to calculate how the feed rate can be maximized considering the capabilities of a given machine tool by following the path from point to point. However, if the limits are exceeded along the deceleration segments, iterative backward steps would be required to correct the feed rate function. To avoid multiple recalculations of feasible feed rate, the use of a bidirectional scanning technique is suggested [53]. With this solution, a backward scanning process is performed to control the decelerations, followed by a forward scanning process to control the accelerations. In this technique, the tangential acceleration limitation can be performed in two steps but without repeated backward steps.

2.3 Applying multiple constraints in feed rate scheduling

Applying multiple constraints in feed rate scheduling requires a multi-step process. After determining the tool path, the following steps are required to perform:

Step 1 Determining the cutter engagement and curvature radius along tool path
Step 2 Calculating the equivalent feed rate based on cutter engagement
Step 3 Calculating the centripetal acceleration and decreasing feed rate locally, if necessary
Step 4 Calculating the tangential acceleration using backward scanning and decreasing the feed rate locally, if necessary
Step 5 Calculating the tangential acceleration using forward scanning and decreasing the feed rate locally, if necessary
Step 6 Generating the segments of NC program with adjusted feed rate

The implementation of these steps will be illustrated by a practical example in Section 3.4.

3 Practical examples

For investigating the feed rate scheduling methods detailed in Section 2, several cutting experiments were performed. First, a preliminary experiment was required to generate sample data for the equivalent feed rate models. Then, the reliability of developed models was examined trough a

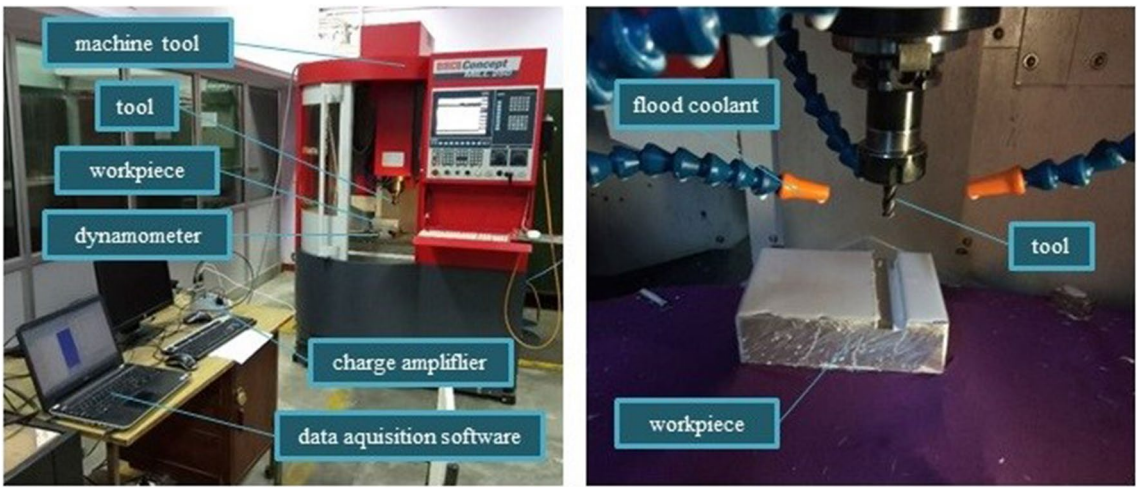

Fig. 5 The experimental setup for the cutting tests

straight milling experiment. Finally, the complete feed rate scheduling method was tested during a trochoidal milling operation.

3.1 Experimental setup

The cutting experiments were performed on an EMCO Concept Mill 250 3-axis machining centre with a Sinumerik 840D controller (refer to Fig. 5). The acceleration capabilities of sleds were $a_{max} = 100\,\frac{mm}{s^2} = 0.01\,g$ both in centripetal and tangential direction. The tool was a solid carbide end mill (tool type: Totem, FBK0500726) with TiAlN coating, the tool diameter (d) was $\varnothing 8mm$, the number of teeth (z) was 4, and helix angle (λ) was 30°. To minimize the effect of tool wear, an easy-to-machine aluminium alloy (Al7075) was chosen for workpiece material.

The cutting parameters have been set according to the tool catalogue. The cutting speed (v_c) was 100 m⁄min, so the spindle speed (n) was 3980 rpm. The feed rate (v_f) was calculated according to the maximum chip thickness, so it varied between 200 and 3000 mm⁄min depending on the cutter engagement. When choosing the cutter engagement, the focus was on the range between 15° and 75°, which is typical in trochoidal milling. In the case of helical tool edge design, the axial depth of cut also affects the characteristics of cutting force evolution. Trochoidal milling is primarily characterized by high axial depths of cut. However, it was also worth investigating how the developed method performs with small cutting depths. Therefore, two different settings have been investigated, namely, $a_p = d/4 = 2$ and $a_p = d = 8mm$.

During the experimentation, the cutting force was measured with a Kistler 9257BA-type piezoelectric dynamometer. For data acquisition, the Labview software was used. The sampling frequency was 25600 Hz (~385 measured points per tool revolution). The force components were measured separately for each coordinate axis. In the evaluation, the maximum force in a tool revolution was analysed in the machining plane (XY) since this component is the determining factor in terms of tool load and machining energy demand. The resulting force was calculated according to Eq. (17):

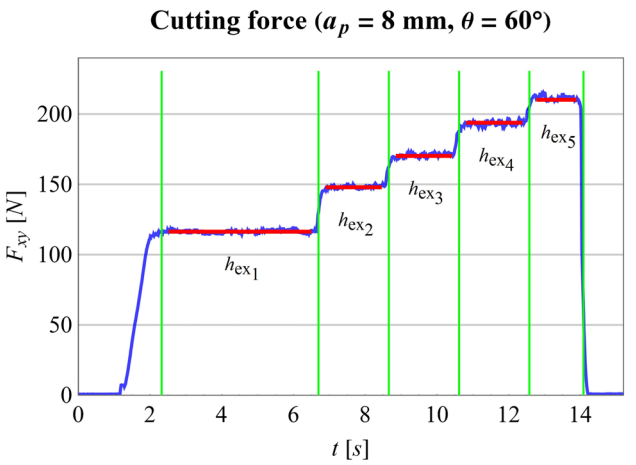

Fig. 6 The measured cutting forces at one cutter engagement

$$F_{xy} = \sqrt{{F_x}^2 + {F_y}^2}[N] \tag{17}$$

where F_x and F_y are the force components per axis. In the following, the designation F_{xy} will refer to the maximum force within one tool revolution.

3.2 Preliminary experiments for configuring the feed rate models

To generate sample data for the force-based equivalent feed rate models, preliminary experiments with straight milling were performed at different cutter engagements and feed rates.

3.2.1 Measured data

During the preliminary cutting experiments, a full factorial experiment was performed with two depths of cut, twelve cutter engagements, and five feed rates. This means a total of 120 settings, but the different feed rates could be examined within one measurement, so only 24 straight milling sections was necessary. The feed rates for each cutter engagement were determined separately to have consistent maximum chip thicknesses with five uniformly increasing values. The

Table 1 Cutting parameters for the preliminary experiments

Factors			Levels
a_p	Axial depth of cut	mm	2, 8 (2 levels)
θ	Cutter engagement	°	15, 20, 25, 30, 35, 40, 45, 50, 55, 60, 65, 70 (12 levels)
h_{ex}	Maximum chip thickness	mm	0.012, 0.024, 0.036, 0.048, 0.06 (5 levels)

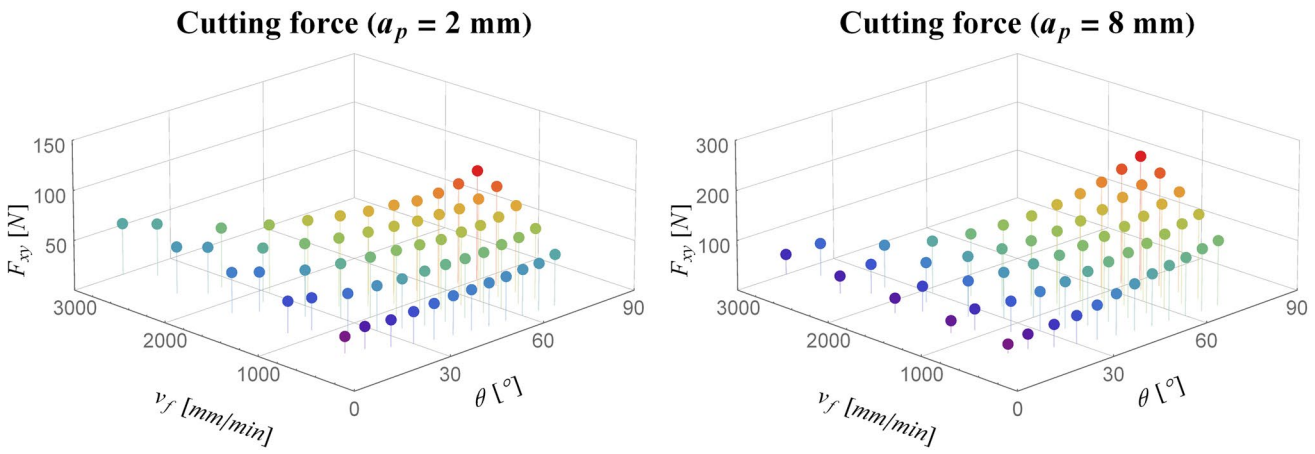

Fig. 7 The measured cutting forces at different cutter engagements and feed rates

parameter settings used during the experiment are summarized in Table 1.

The cutting force measured at one milling segment is illustrated in Fig. 6. Because the cutting force definitely increased with the increasing feed rate, measuring the different feed rate settings within one segment did not cause any problem since the sections could be easily separated. The cutting force for a given parameter combination was determined by calculating the arithmetic mean within a section, disregarding the outer parts of the range.

The results of preliminary experiments are shown in Fig. 7. A nonlinear relationship between the cutting parameters and the measured cutting force could be observed for both axial depths of cut. This nonlinear trend could not be eliminated either by replacing the cutter engagement with radial depth of cut or the feed rate with chip thickness. Therefore, this phenomenon must be dealt with when modelling the equivalent feed rate.

3.2.2 Equivalent feed rate models

The process for modelling the equivalent feed rate is shown in Fig. 8. At first, the formula $v_{f,eq}(F,\theta)$ must be determined based on the measured sample data. Later, based on the reference point corresponding to nominal input parameters, it can be specified how to adjust the feed rate as a function of cutter engagement in order to keep the cutting force constant. In other words, if the bivariate regression model $v_{f,eq}(F,\theta)$ is available, fixing the value of F gives a simple univariate relationship for controlling the feed.

The regression models were created separately for the two different axial depths of cut. The formulas gained after substituting the constant parameters determined by the method of least squares are summarized in Table 2.

The coefficient of determination $\left(R^2\right)$ is often used to quantify the goodness of regression models. This parameter can express how well the regression model

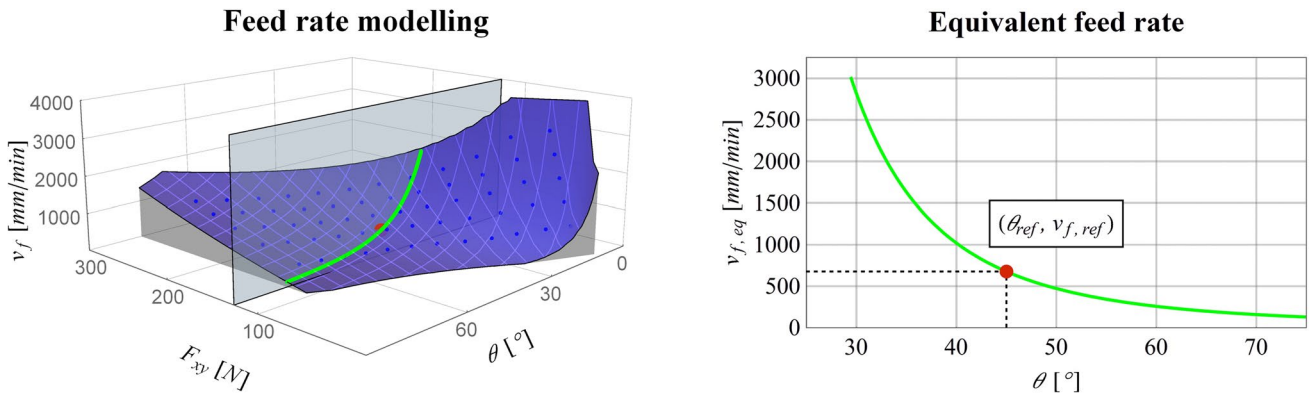

Fig. 8 Calculating the equivalent feed rate based on a regression model $\left(a_p = 8mm, \theta_{ref} = 45°, F_{xy,ref} = 125N\right)$

Table 2 The calculated regression model parameters

$a_p[mm]$	Regression model	Formula $[mm/min]$
2	*second order* $v_{f,reg_{2nd}}(F,\theta)$	$1.259 \bullet 10^3 + 6.537 \bullet 10^1 F - 1.143 \bullet 10^2 \theta + 9.684 \bullet 10^{-2} F^2 + 1.495\theta^2 - 1.033 F\theta$
	third order $v_{f,reg_{3rd}}(F,\theta)$	$1.004 \bullet 10^3 + 7.575 \bullet 10^1 F - 1.198 \bullet 10^2 \theta + 9.423 \bullet 10^{-1} F^2 + 4.118\theta^2 - 4.172 F\theta - 4.923 \bullet 10^{-3} F^3 - 3.176 \bullet 10^{-2} \theta^3 + 4.291 \bullet 10^{-3} F^2 \theta + 2.686 \bullet 10^{-2} F\theta^2$
	exponential $v_{f,reg_{exp}}(F,\theta)$	$-5.103 \bullet 10^2 + 7.413 \bullet 10^2 F^{1.181} \theta^{-1.134}$
8	*second order* $v_{f,reg_{2nd}}(F,\theta)$	$3.717 \bullet 10^3 + 5.516 \bullet 10^1 F - 2.673 \bullet 10^2 \theta + 6.855 \bullet 10^{-3} F^2 + 3.136\theta^2 - 7.802 \bullet 10^{-1} F\theta$
	third order $v_{f,reg_{3rd}}(F,\theta)$	$6.215 \bullet 10^3 + 1.272 \bullet 10^2 F - 6.692 \bullet 10^2 \theta + 2.664 \bullet 10^{-1} F^2 + 1.875 \bullet 10^1 \theta^2 - 5.370 F\theta - 4.306 \bullet 10^{-4} F^3 - 1.425 \bullet 10^{-1} \theta^3 + 4.701 \bullet 10^{-5} F^2 \theta + 4.146 \bullet 10^{-2} F\theta^2$
	exponential $v_{f,reg_{exp}}(F,\theta)$	$7.305 \bullet 10^1 + 1.130 \bullet 10^4 F^{2.143} \theta^{-3.460}$

approximates the real data points. Its value can be calculated as follows:

$$R^2 = 1 - \frac{\sum_i \left(y_i - \hat{y}_i\right)^2}{\sum_i \left(y_i - \bar{y}\right)^2} \tag{18}$$

where y_i are the input feed rates of experiment, $\hat{y}_i$ are the output feed rates calculated by regression model, and $\bar{y}$ is the mean of input feed rate parameters.

The differences between the input values of measurement and the output values obtained from regression models are illustrated in Fig. 9. The R^2 parameters calculated from the sample data used in model fitting are also indicated on the diagrams. The residuals were the smallest in the case of ANN-based model; the level of fit of this model was almost perfect:

When analysing the traditional regression models, it can also be concluded that the third-order model outperformed the second-order and exponential regression formulas. However, it must be remarked that the high number of free variables resulted in overfitting; thus, the third-order model showed strong fluctuations between the measured points. This phenomenon occurs particularly at the periphery of the investigated parameter range, where linear regression models have proven unreliable (refer to Fig. 10). At a low cutting force limit, the equivalent feed rate calculated by the formula could even have a negative sign, which is nonsense. Since the exponential formula approximated the nature of the relationship between input and output data better, this formula was chosen for further experiments.

Besides the analytical comparison of regression models, the results obtained for input variables other than the sample data are also worth examining. Furthermore, the models obtained for equivalent feed rate should also be compared with the geometry-based models. These comparisons were not feasible directly, so another experiment was required. The results of that experiment are described in the following subsection.

3.3 Testing the feed rate models in straight milling

Before the trochoidal milling experiments, the feed rate models were tested under simpler conditions. In order to verify the adequacy of the models, measurements with straight milling were performed. As the polynomial models showed overfitting, only the exponential regression model was examined beside the ANN-based model. The number of methods to be tested has also been reduced for the geometric methods. Although Eq. (8) and Eq. (9) differ significantly from each other, the difference between the average chip thickness obtained with the two formulas is small at low cutter engagements. Therefore, only the first formula was tested in the experiments because the cutter engagement will remain low in trochoidal milling, too. Thus, five approaches were compared: three geometric methods (constant h_{ex}, h_m, or MRR), the exponential regression model, and the ANN-based model.

For the reference point of comparison, the cutter engagement was $\theta_{ref} = 45°$, and the feed rate was calculated for a maximum chip thickness of $h_{ex} = 0.05mm$ which resulted in $v_{f,ref} = 796mm/min$. With these reference values, a wide range of feed rates could be scrutinized. Experiments were performed for both 2 mm and 8 mm axial depths of cut. The other cutting parameters were the same as in the preliminary experiment.

The results of the experiments are summarized in Fig. 11. The experimentation confirmed the assumption that the tool load cannot be kept constant by using the geometric methods. When controlling the chip thickness, even a multiple increase

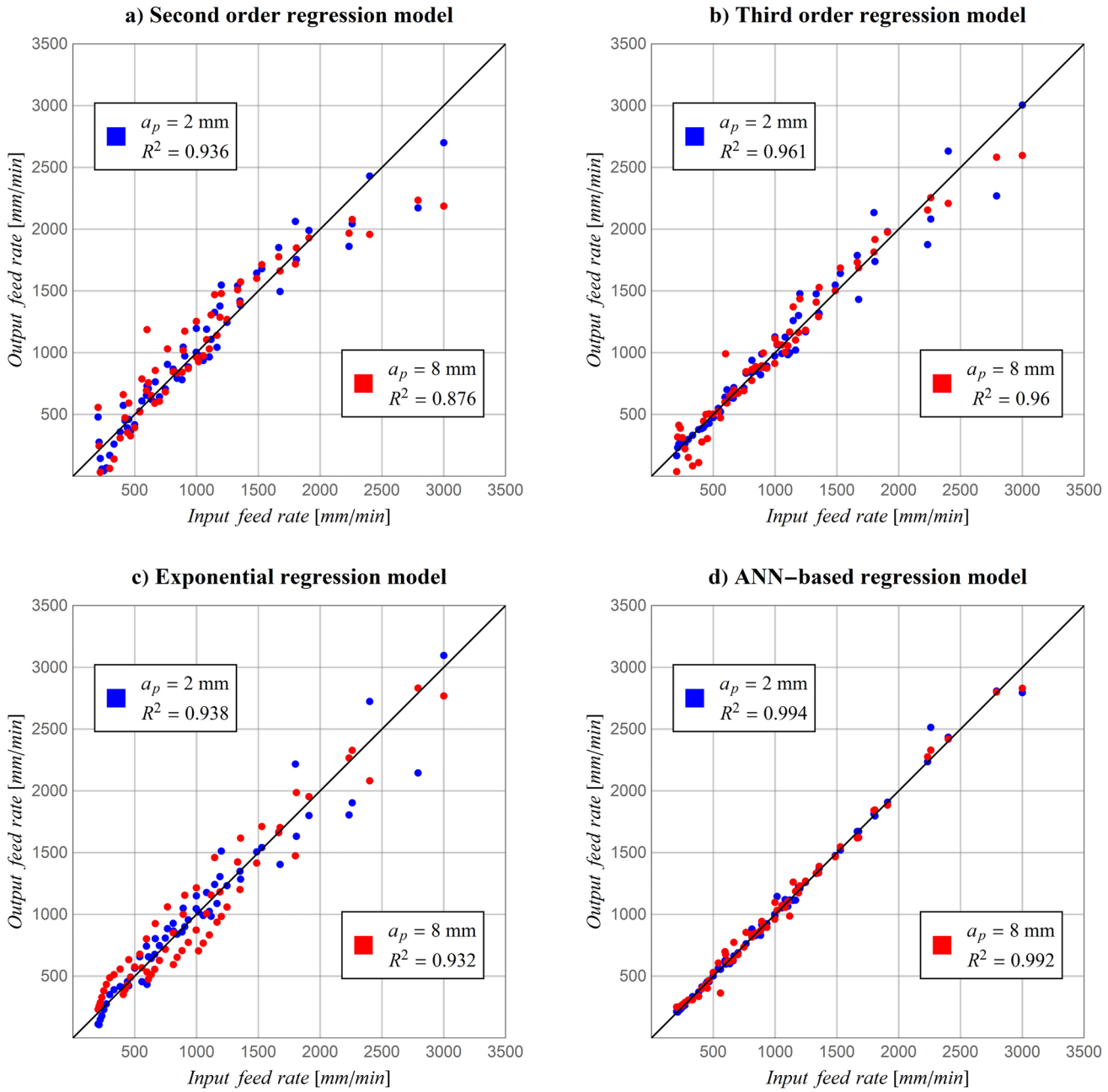

Fig. 9 Analytical comparison of the different regression models: **a**) second order regression, **b**) third order regression, **c**) exponential regression, **d**) ANN-based regression

in cutting force was observed in the examined cutter engagement range. Controlling the MRR provided slightly better results, especially in the case of smaller depths of cut. In this experiment, by using geometric methods, a lower cutting force was measured if the cutter engagements were smaller than the nominal, while a higher cutting force was measured if the cutter engagements were larger than the nominal. This deviation will lead to the following consequences. The decreased cutter engagement results in a waste of time, as the tool moves slower than permitted. On the contrary, the increased cutter engagement can lead to overloading, adversely affecting both tool life and machining quality. Furthermore, there is no guarantee that the same trend will occur with other tools or settings, so introducing a safety factor cannot solve the problem.

In contrast, the experimental-based methods were more reliable. Their application can ensure a minimum machining

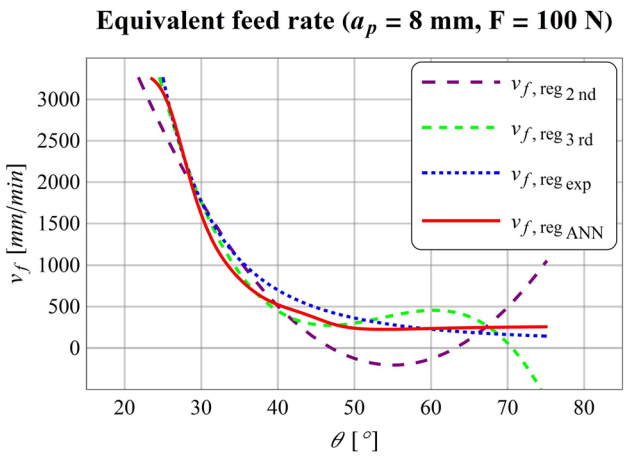

Fig. 10 The problematic operation of linear regression models at the investigated parameter range's periphery

time while keeping the cutting force under control. It can also be noticed that the ANN-based solution worked excellently for both axial depths of cut (the maximum relative errors were 3.1% and 2.9%), while the exponential regression model showed slight fluctuations in cutting force (the maximum relative errors were 14.1% and 4.4%), which already stretches the limit of acceptability.

In straight milling, the accelerations have not played any role. This aspect will be scrutinized in the following example, where the trochoidal milling was examined.

3.4 Testing the feed rate scheduling method in trochoidal milling

To investigate the different feed rate models, trochoidal milling experiments were performed. During the experiments, straight slots with different widths ($b = 12, 16, 20mm$) were machined. In trochoidal milling, the acceleration constraints also need to be addressed, so all steps of feed rate scheduling can be presented in that example.

In order to get a more comprehensive picture of feed models, a different reference point was used than during the straight milling experiments since; due to acceleration

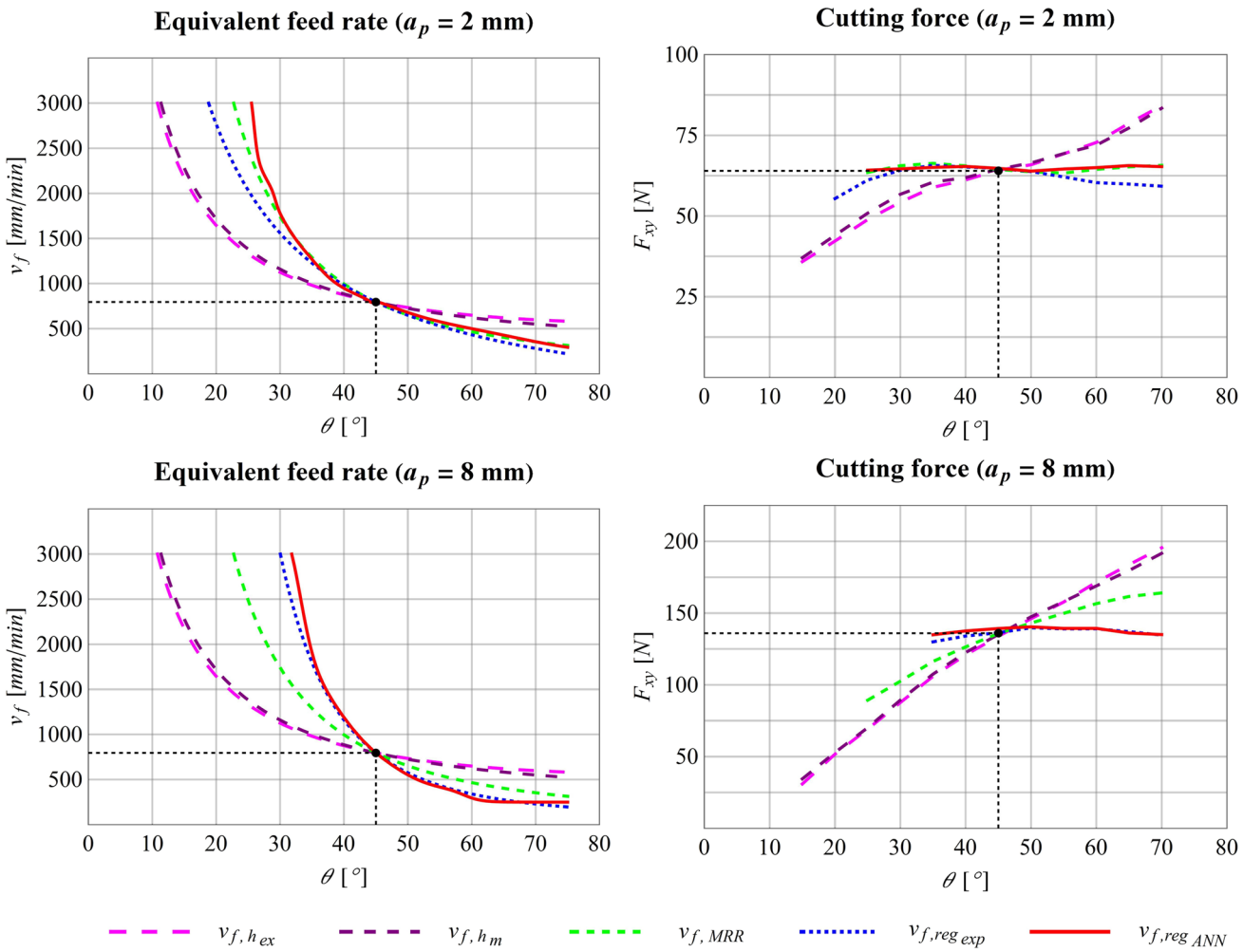

Fig. 11 Experimental comparison of the different regression models

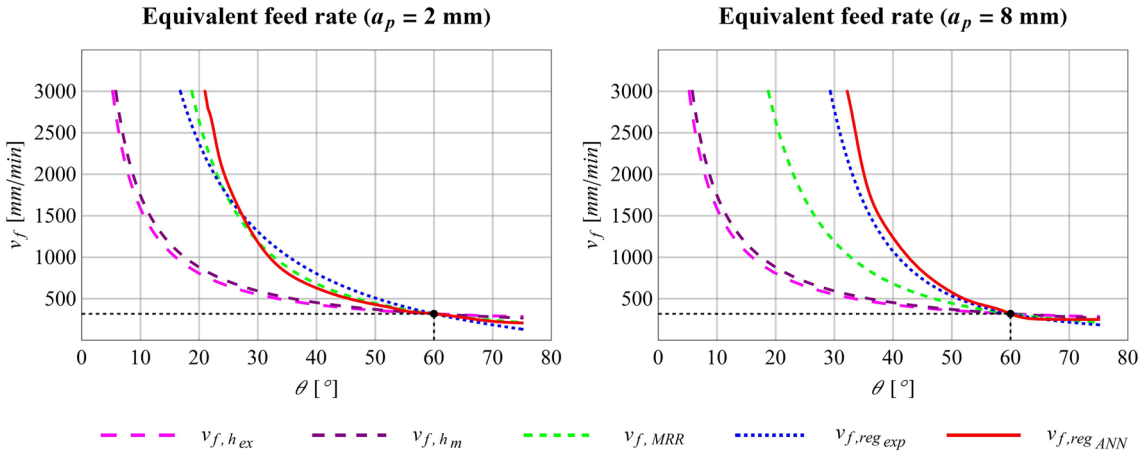

Fig. 12 Equivalent feed rates for the reference parameter used at trochoidal milling

limitations, it was only possible to investigate lower feed rates. Furthermore, the characteristic of trochoidal milling is that the nominal cutter engagement limits the instantaneous value from above. Therefore, the reference cutter engagement was increased to $\theta_{ref} = 60°$, and the reference maximal chip thickness was reduced to $h_{ex} = 0.02mm$, which resulted in a feed rate of $v_{f,ref} = 318mm/min$. The other parameters, namely, the axial depths of cut, the cutting speed, the workpiece, the tool, and the machine tool, remained the same. The equivalent feed rates for that reference point are shown in Fig. 12. Since the trochoidal tool path was generated so that the cutter engagement reaches the reference value (60°) at the maximum immersion, the range below the reference value should be considered. When analysing Fig. 12, it can be concluded that keeping the average or maximum chip thickness constant gives a lower feed rate than the permissible at both axial depths of cut. In case of a low axial depth of cut $(a_p = 2mm)$, keeping the MRR constant gave almost the same results as the experimental-based methods. However, in case of a larger axial depth of cut $(a_p = 8mm)$, the feed rate with constant MRR was also lower than the permissible. The extent to which this lower feed rate increases the machining time compared to experimental-based models will be detailed later.

Before analysing the evolution of machining time, Fig. 13 shows the steps of feed rate scheduling. The horizontal axis of the diagrams corresponds to the arc length travelled along the tool path. In the methods described in Sect. 2, the tool path shape must be given as an input data. The figure shows a cycloidal tool path generated for a $b = 12mm$ wide slot using a tool diameter of $d = \varnothing 8mm$ with a maximum cutter engagement of $\theta_{ref} = 60°$.

Once the tool path is known, the first step of feed rate scheduling is to determine the cutter engagement and curvature radius at discrete points along the tool path. To accomplish this, a self-developed simulation algorithm was used [54]. Based on the diagram of cutter engagement, it can be stated that the nominal immersion lasts only for a moment, while the rolling-in and out sections take place over a long time. This feature makes the feed rate scheduling necessary if the goal is to achieve maximum productivity. Although the curvature radius fluctuates only slightly, which is one of the main advantages of cycloidal strategy, the centripetal acceleration will still significantly limit the feasible feed rate, as seen later.

After calculating the trajectory-specific data, the second step of feed rate scheduling is to assign the equivalent feed rate to tool path points based on the calculated cutter engagements. Since the equivalent feed rate goes to infinity if the cutter engagement is close to zero, it is advisable to specify a maximum value for the feed rate. During the experiments, the limit was selected for $v_{f,max} = 1500mm/min$. However, even this feed rate was not available regarding the centripetal acceleration. The diagram of accelerations shows that the machine tool's $a_{max} = 100\frac{mm}{s^2} = 0.01g$ acceleration capabilities were small for both centripetal and tangential acceleration. Therefore, a reduction in feed rate is required.

The third step in feed rate scheduling is to reduce the feed where the centripetal acceleration has exceeded the machine tool's capabilities. The diagram shows that this required a significant reduction, but the tangential acceleration remained still too high on some segments. After the next two steps of feed rate scheduling, by reducing the feed on the critical sections through firstly a backward and secondly a forward scanning operation, the constraints of tangential acceleration can also be met. After the fifth step, the corresponding feed rates are available at discrete points along the tool path, based on which the NC program can be created using short segments with variable feed rates.

Figure 14 shows the evolution of cutting force with different feed rate scheduling methods. As a reference, an experiment was also performed with a constant feed rate. Although

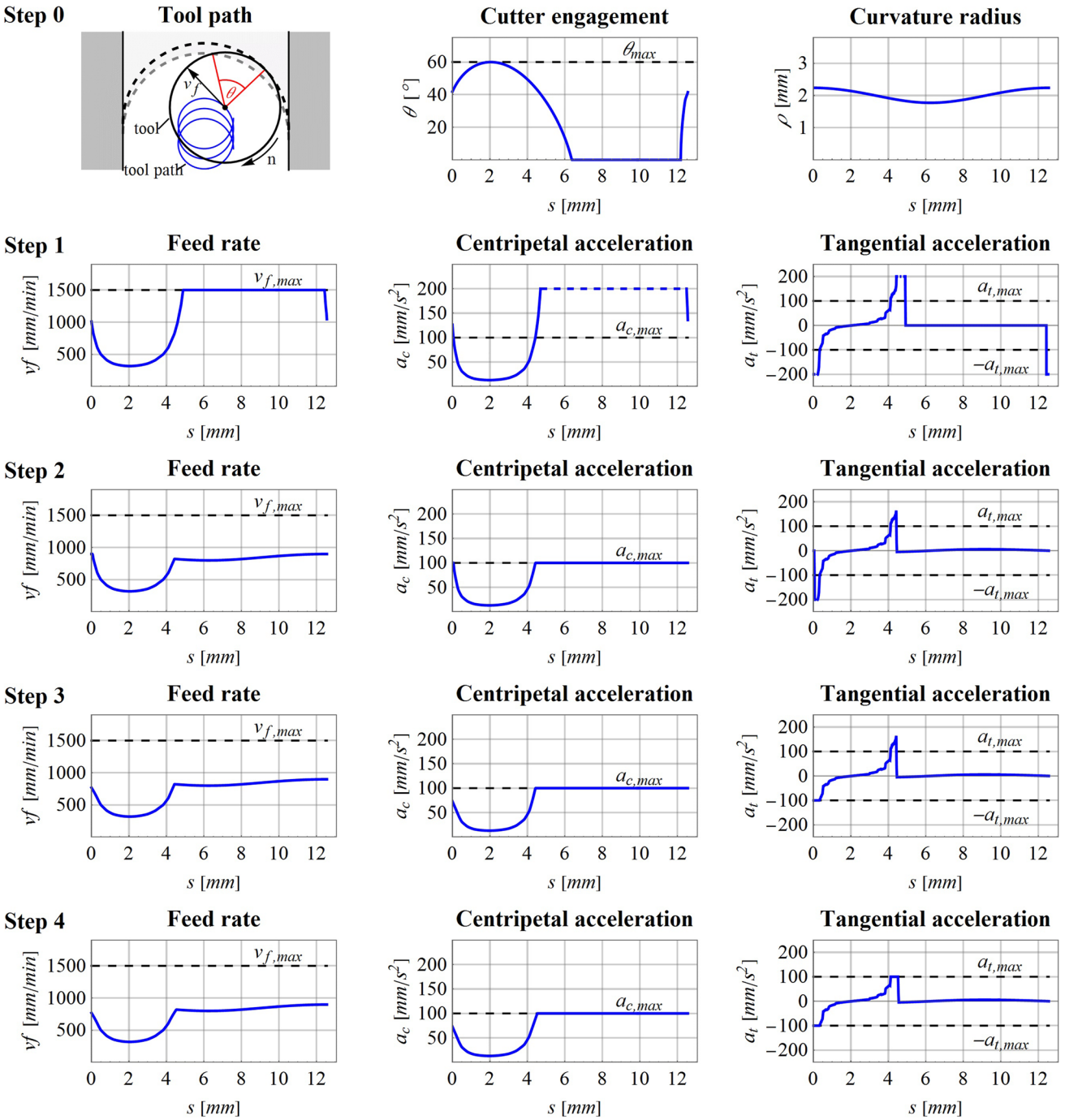

Fig. 13 The feed rate and acceleration functions after each steps of feed rate scheduling

a few per cent fluctuations can be observed in the peaks of cutting force, this is impossible to avoid due to the complexity of cutting process. On the one hand, the input data used when creating the equivalent feed rate models were produced by straight-line milling, while in trochoidal milling, the tool moved along an arc. This difference also affects how the coolant reaches the cutting zone. On the other hand, specifying the path in small segments also means that the actual feed rate and cutter engagement can slightly differ from the calculated value. Despite all this, there was only a few per cent difference between the maximum cutting forces, which is acceptable.

The diagrams in Fig. 14 show that the tool entering and exiting takes a long time without feed rate scheduling, where the tool does not work at maximum efficiency. It can be noted that only the experimental-based models were able to maintain the cutting force level, primarily the method using ANN. In

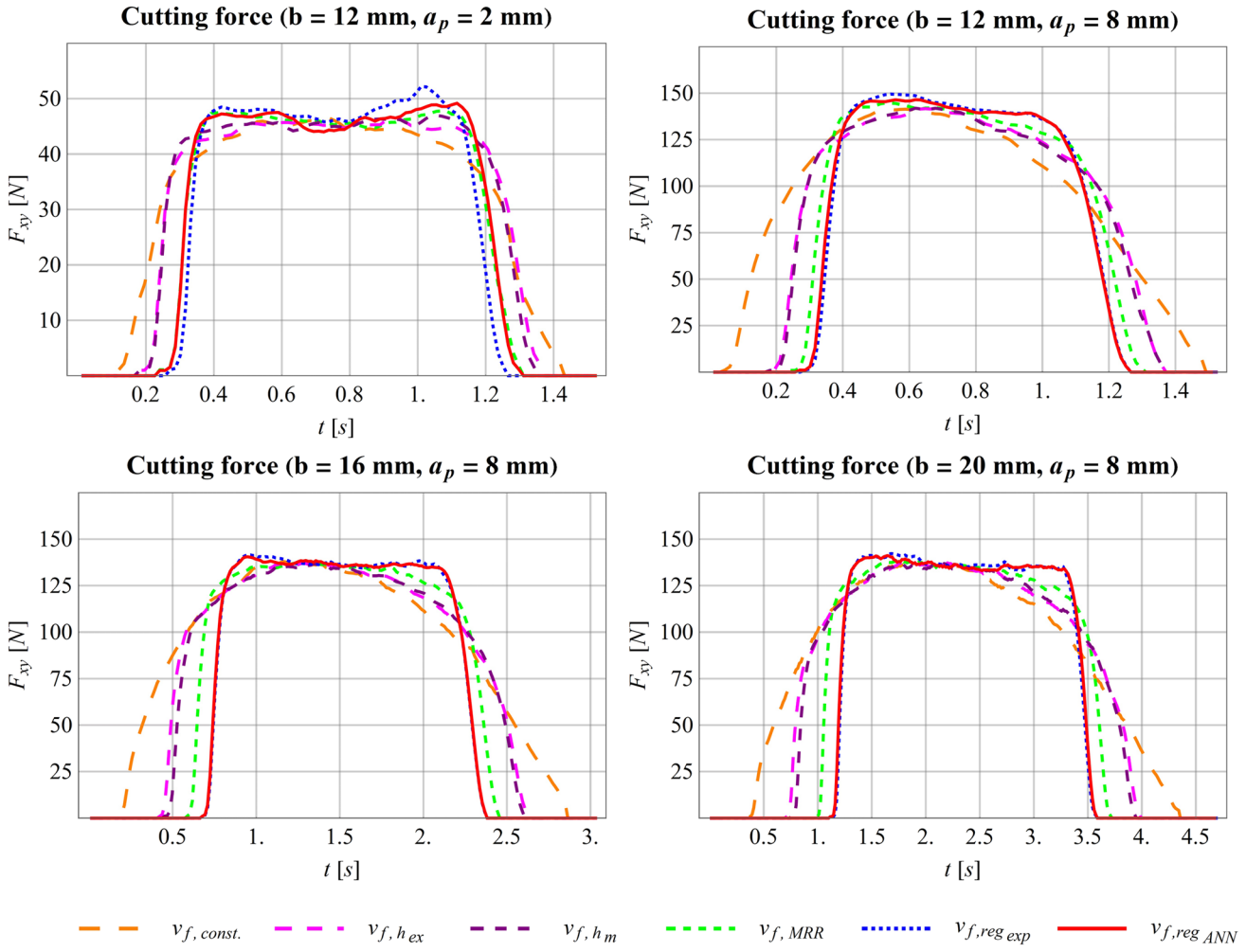

Fig. 14 The evolution of cutting force with different feed rate scheduling methods at trochoidal milling

the experiments with a cutting depth of 8 mm, the maximum cutting force was only marginally higher (0.9–2.2%) with the regression formula than with the ANN-based approach. However, with a cutting depth of 2 mm, the difference was a non-negligible 6.1% in favour of the latter method. Geometric methods were also more favourable compared the cases where constant feed rate were used, but these approaches could only partially address the problem of changing cutting conditions. The shortcomings of these methods are mainly due to the longer machining time compared to the experimental feed rate scheduling methods. By increasing the slot width, the benefit of experimental methods also increased slightly since the length of transitional segments become even longer, and the centripetal acceleration was less restrictive because of the larger path curvature radius.

Table 3 summarizes the machining times obtained using different feed rate scheduling methods in the previous cutting experiment. The values given refer to one trochoidal period. The period times were determined both by simulation and by experiment. During the simulation, the tool path can be divided into as many short sections as wanted in feed rate scheduling. Therefore, a more accurate result can be obtained. However, on the machine tool's controller used in the experiments, it was necessary to provide a time of at least 15 ms for each motion segment to ensure continuous program execution, so only a coarser resolution could be used. As a result, the experimentally determined time was a few per cent longer. However, the differences were the same when comparing the strategies relative to each other.

In the comparison, the machining with constant feed rate was the reference $\left(v_{f,const}\right)$. This choice was justified because feed rate scheduling is rarely used in trochoidal machining since the cutter engagement fluctuates only slightly. Firstly, the extent to which the period time can be reduced if an increased feed rate is applied for the linking segments was examined $\left(v_{f,const^*}\right)$. Despite the shortness of linking segments, the results show that this improvement alone resulted in a 27–35% machining time reduction. However, this can

Table 3 Effect of feed rate scheduling method on machining time at different slot widths

Slot width	Method	Simulation				Cutting experiment	
		Cutting time	Linking time	Period time	Improvement	Period time	Improvement
$b[mm]$	$[-]$	$t_{c,sim}[s]$	$t_{l,sim}[s]$	$t_{p,sim}[s]$	[%]	$t_p[s]$	[%]
12	$v_{f,const}$	1.270	1.098	2.368	-	2.49	-
	$v_{f,const^*}$	1.270	0.467	1.737	26.6	1.86	25.3
	$v_{f,h_{ex}}$	1.035	0.420	1.455	38.6	1.55	37.9
	v_{f,h_m}	1.011	0.418	1.430	39.6	1.53	38.5
	$v_{f,MRR}$	0.895	0.413	1.308	44.8	1.39	44.3
	$v_{f,reg_{exp}}$	0.819	0.412	1.231	48.0	1.30	47.7
	$v_{f,reg_{ANN}}$	0.827	0.412	1.239	47.7	1.32	47.1
16	$v_{f,const}$	2.516	2.218	4.734	-	5.07	-
	$v_{f,const^*}$	2.516	0.696	3.212	32.2	3.42	32.4
	$v_{f,h_{ex}}$	2.038	0.606	2.644	44.1	2.81	44.3
	v_{f,h_m}	1.985	0.604	2.589	45.3	2.76	45.5
	$v_{f,MRR}$	1.710	0.589	2.300	51.4	2.46	51.5
	$v_{f,reg_{exp}}$	1.527	0.588	2.115	55.3	2.26	55.4
	$v_{f,reg_{ANN}}$	1.540	0.588	2.128	55	2.26	55.4
20	$v_{f,const}$	3.744	3.356	7.100	-	7.16	-
	$v_{f,const^*}$	3.744	0.877	4.621	34.9	4.68	34.6
	$v_{f,h_{ex}}$	3.028	0.754	3.782	46.7	3.84	46.4
	v_{f,h_m}	2.947	0.750	3.697	47.9	3.74	47.8
	$v_{f,MRR}$	2.509	0.729	3.237	54.4	3.28	54.2
	$v_{f,reg_{exp}}$	2.214	0.728	2.942	58.6	2.99	58.2
	$v_{f,reg_{ANN}}$	2.233	0.728	2.961	58.3	3.00	58.0

be further enhanced if the equivalent feed rate is used in the cutting segments.

The benefits of feed rate scheduling can be seen in two respects. Firstly, the travelling time required for the cutting segment will be reduced. Secondly, at the same time, the travelling time of linking segment will also be decreased since that movement can start and end at a higher speed. As a result, the period time was further reduced by 10–20% in the sample examined. In the comparison, the experimental-based models provided the best results, with a 48–58% reduction in machining time compared to the strategy with a constant feed rate. In this experiment, the exponential approximation formula slightly outperformed the ANN-based method by a few tenths of a per cent in terms of machining time. However, considering that this was accompanied by a greater increase in maximum cutting force, the latter method is preferable. Furthermore, the ANN-based method performed also better in cutting force control during the straight milling experiments, which also justifies the preference for the ANN-based method.

The experiment confirmed the expectation that even in trochoidal milling, machining productivity can be significantly increased by adjusting the feed rate. Even though the cutter engagement fluctuates in a narrow range, it is worth paying attention to this area because, without it, significant reserves may remain untapped. Furthermore, the experiments also demonstrated that it is sufficient to focus only on the force maxima when scheduling the feed rate, which significantly simplifies the determination of model parameters.

4 Conclusion

In this paper, the traditional geometric and regression-based methods and a newly developed ANN-based feed rate scheduling algorithm were experimentally and theoretically compared under straight and trochoidal milling conditions. The results showed that the tool load can better be controlled through the developed ANN-based method. This is important for maintaining machining quality, avoiding premature tool wear, and optimizing machining time. The consideration of acceleration constraints supports the practical application of the proposed method. The case studies demonstrated the reliability and efficiency of the developed technique for both straight milling and trochoidal milling.

Based on the comparative study, the following conclusions can be drawn:

- Geometric models can only partially handle the changing cutting conditions in terms of controlling the tool load.

- With the experimental-based equivalent feed rate models, the effect of axial depth of cut can also be considered, in contrast to chip thickness and MRR-based methods.
- ANN-based equivalent feed model can outperform the models constructed with traditional regression techniques in terms of reliability and accuracy.
- In trochoidal milling experiments, around 50% reduction in machining time was achieved by applying the developed feed rate scheduling method as compared to using a constant feed rate.

Despite the convincing results, there is still scope for further improvement. When defining the equivalent feed model, some fixed parameters can be changed to free variables, such as cutting speed and axial depth of cut. Furthermore, it would be worthwhile to examine tools with more complex geometries, such as bull nose end mill. In that case, more additional variables should be considered when creating the ANN-based feed rate scheduling model because the tool orientation could also significantly affect the evolving cutting force. However, there are no obstacles to implementing these enhancements, as neural networks can be applied as universal regression models.

Acknowledgements The authors would like to show gratitude to the Manufacturing Science Laboratory, Department of Mechanical Engineering, Indian Institute of Technology Kanpur, Kanpur, UP India, especially to Mr Sanjeev Kumar Verma and Mr Atul Kumar Gangwar, for their indispensable assistance in conducting the experiments. The research would also not have been possible without the help of the Department of Mechanical Engineering, Amity University Uttar Pradesh, Noida, UP India.

Author contribution All authors contributed to the study conception and design. Material preparation, data collection, and analysis were performed by Adam Jacso. The first draft of the manuscript was written by Adam Jacso and Rajeev Kumar Singh, and all authors commented on previous versions of the manuscript. All authors read and approved the final manuscript.

Funding Open access funding provided by Budapest University of Technology and Economics. The research reported in this paper and carried out at BME has been supported by the NRDI Fund (TKP2020 NC, Grant No. BME-NC) based on the charter of bolster issued by the NRDI Office under the auspices of the Ministry for Innovation and Technology. The work for this paper was supported by the European Commission through the H2020 project EPIC under grant No. 739592, the 2017–1.3.1-VKE-2017–00029 grant of the Hungarian National Research, Development and Innovation Office (NKFIH), and the Hungarian State Eötvös Scholarship.

Declarations

Competing interests The authors declare no competing interests.

References

1. Jacso A, Szalay T (2018) Analysing and optimizing 2.5D circular pocket machining strategies. Lect Notes Mech Eng (201519). https://doi.org/10.1007/978-3-319-68619-6_34
2. Tang L, Landers RG (2012) Predictive contour control with adaptive feed rate. IEEEASME Trans Mechatron17:4. https://doi.org/10.1109/TMECH.2011.2119324
3. Chen J, Ren F, Sun Y (2016) Contouring accuracy improvement using an adaptive feedrate planning method for CNC machine tools. Procedia CIRP 56:299–305. https://doi.org/10.1016/j.procir.2016.10.012
4. Du X, Huang J, Zhu LM (2015) A complete S-shape feed rate scheduling approach for NURBS interpolator. J Comput Des Eng 2(4):206–217. https://doi.org/10.1016/j.jcde.2015.06.004
5. Du X, Huang J, Zhu LM (2015) A complete S-shape feed rate scheduling approach for NURBS interpolator. J Comput Des Eng 2:4. https://doi.org/10.1016/j.jcde.2015.06.004
6. Huang J, Du X, Zhu LM (2019) Parallel acceleration/deceleration feedrate scheduling for computer numerical control machine tools based on bi-directional scanning technique. Proc Inst Mech Eng Part B J Eng Manuf 233:3. https://doi.org/10.1177/0954405417706997
7. Fan W, Fang C, Ye P, Shi S, Zhang X (2015) Convex optimisation method for time-optimal feedrate planning with complex constraints. Proc Inst Mech Eng Part B J Eng Manuf 229:1. https://doi.org/10.1177/0954405414558698
8. Li H, Wang W, Li Q, Huang P (2019) A novel minimum-time feedrate schedule method for five-axis sculpture surface machining with kinematic and geometric constraints. Proc Inst Mech Eng Part B J Eng Manuf 233: 5. https://doi.org/10.1177/0954405418780167
9. Pessoles X, Redonnet J-M, Segonds S, Mousseigne M (2012) Modelling and optimising the passage of tangency discontinuities in NC linear paths. Int J Adv Manuf Technol 58(5):631–642. https://doi.org/10.1007/s00170-011-3426-z
10. Li Z, Yan Q, Tang K (2021) Multi-pass adaptive tool path generation for flank milling of thin-walled workpieces based on the deflection constraints. J Manuf Process 68:690–705. https://doi.org/10.1016/j.jmapro.2021.05.075
11. Swetangkumar Bavaramanandi, Patel Divyang D, Dodiya Hardik R (2019) A brief review on feed rate optimization and different type of toolpath use in pocket machining. Int J Tech Innov Mod.Eng Sci 5(3):8
12. Xiong G, Li Z-L, Ding Y, Zhu L (2020) Integration of optimized feedrate into an online adaptive force controller for robot milling. Int J Adv Manuf Technol 106:3. https://doi.org/10.1007/s00170-019-04691-1
13. Ridwan F, Xu X, Ho FCL (2012) Adaptive execution of an NC program with feed rate optimization. Int J Adv Manuf Technol 63:9. https://doi.org/10.1007/s00170-012-3959-9
14. Ibaraki S, Shimizu T (2010) A long-term control scheme of cutting forces to regulate tool life in end milling processes. Precis Eng 34(4):675–682. https://doi.org/10.1016/j.precisioneng.2010.05.001
15. Kim D, Jeon D (2011) Fuzzy-logic control of cutting forces in CNC milling processes using motor currents as indirect force

sensors. Precis Eng 35(1):143–152. https://doi.org/10.1016/j.precisioneng.2010.09.001
16. Liu X, Ding Y, Yue C, Zhang R, Tong X (2016) Off-line feedrate optimization with multiple constraints for corner milling of a cavity. Int J Adv Manuf Technol 82:9. https://doi.org/10.1007/s00170-015-7469-4
17. Bae S-H, Ko K, Kim BH, Choi BK (2003) Automatic feedrate adjustment for pocket machining. Comput-Aided Des 35:5. https://doi.org/10.1016/S0010-4485(01)00195-6
18. Biró I, Szalay T (2017) Extension of empirical specific cutting force model for the process of fine chip-removing milling. Int J Adv Manuf Technol 88:9–12. https://doi.org/10.1007/s00170-016-8957-x
19. Su S, Zhao G, Xiao W, Yang Y, Cao X (2021) An image-based approach to predict instantaneous cutting forces using convolutional neural networks in end milling operation. Int J Adv Manuf Technol 115(5):1657–1669. https://doi.org/10.1007/s00170-021-07156-6
20. Ma W, Wang R, Zhou X, Xie X (2021) The finite element analysis–based simulation and artificial neural network–based prediction for milling processes of aluminum alloy 7050. Proc Inst Mech Eng Part B J Eng Manuf 235(1–2):265–277 . https://doi.org/10.1177/0954405420932442
21. Bailey T, Elbestawi MA, El-Wardany TI, Fitzpatrick P (2002) Generic simulation approach for multi-axis machining, part 2: model calibration and feed rate scheduling. J Manuf Sci Eng 124(3):634. https://doi.org/10.1115/1.1468864
22. Wei Z, Wang M, Han X (2010) Cutting forces prediction in generalized pocket machining. Int J Adv Manuf Technol 50(5):449–458. https://doi.org/10.1007/s00170-010-2528-3
23. Park H, Qi B, Dang DV, Park DY (2018) Development of smart machining system for optimizing feedrates to minimize machining time. J Comput Des Eng 5(3):299–304. https://doi.org/10.1016/j.jcde.2017.12.004
24. Erdim H, Lazoglu I, Ozturk B (2006) Feedrate scheduling strategies for free-form surfaces. Int J Mach Tools Manuf 46(7–8):747–757. https://doi.org/10.1016/j.ijmachtools.2005.07.036
25. Zhang Z, Luo M, Zhang D, Wu B (2018) A force-measuring-based approach for feed rate optimization considering the stochasticity of machining allowance. Int J Adv Manuf Technol 1–12. https://doi.org/10.1007/s00170-018-2127-2
26. Zhang L, Feng J, Wang Y, Chen M (2009) Feedrate scheduling strategy for free-form surface machining through an integrated geometric and mechanistic model. Int J Adv Manuf Technol 40(11–12):1191–1201. https://doi.org/10.1007/s00170-008-1424-6
27. Farouki RT, Manjunathaiah J, Nicholas D, Yuan GF, Jee S (1998) Variable-feedrate CNC interpolators for constant material removal rates along Pythagorean-hodograph curves. Comput-Aided Des 30(8):631–640. https://doi.org/10.1016/S0010-4485(98)00020-7
28. Kloypayan J, Lee YS (2002) Material engagement analysis of different endmills for adaptive feedrate control in milling processes. Comput Ind 47(1):55–76. https://doi.org/10.1016/S0166-3615(01)00136-1
29. Karunakaran KP, Shringi R, Ramamurthi D, Hariharan C (2009) Octree-based NC simulation system for optimization of feed rate in milling using instantaneous force model. Int J Adv Manuf Technol 46(5–8):465–490. https://doi.org/10.1007/s00170-009-2107-7
30. Qian L, Yang B, Lei S (2008) Comparing and combining off-line feedrate rescheduling strategies in free-form surface machining with feedrate acceleration and deceleration. Robot Comput-Integr Manuf 24(6):796–803. https://doi.org/10.1016/j.rcim.2008.03.015
31. Feed rate optimization - VERICUT USA', CGTech, Sep. 03, 2020. https://cgtech.com/feed-rate-optimization . Accessed 3 Sept 2020
32. Kurt M, Bagci E (2011) Feedrate optimisation/scheduling on sculptured surface machining: a comprehensive review, applications and future directions. Int J Adv Manuf Technol 55(9–12):1037–1067. https://doi.org/10.1007/s00170-010-3131-3
33. Zuperl U, Cus F, Reibenschuh M (2011) Neural control strategy of constant cutting force system in end milling. Robot Comput-Integr Manuf 27(3):485–493. https://doi.org/10.1016/j.rcim.2010.10.001
34. Zuperl U, Cus F, Reibenschuh M (2012) Modeling and adaptive force control of milling by using artificial techniques. J Intell Manuf 23(5):1805–1815. https://doi.org/10.1007/s10845-010-0487-z
35. Xie J et al (2021) Multi-objective feed rate optimization of three-axis rough milling based on artificial neural network. Int J Adv Manuf Technol 114(5):1323–1339. https://doi.org/10.1007/s00170-021-06902-0
36. Rajput AS, Singh A, Kapil S, Das M (2022) Investigations on the trochoidal toolpath for processing the biomaterial through magnetorheological fluid assisted finishing process. J Manuf Process 76:812–827. https://doi.org/10.1016/j.jmapro.2022.02.055
37. Pleta A, Nithyanand G, Niaki FA, Mears L (2019) Identification of optimal machining parameters in trochoidal milling of Inconel 718 for minimal force and tool wear and investigation of corresponding effects on machining affected zone depth. J Manuf Process. https://doi.org/10.1016/j.jmapro.2019.03.048
38. Jacso A, Lado Z, Phanden RK, Sikarwar BS, Singh RK (2022) Bézier curve-based trochoidal tool path optimization using stochastic hill climbing algorithm. Mater Today Proc. https://doi.org/10.1016/j.matpr.2022.12.056
39. Kónya G, Zsolt Kovács F, Kókai E (2022) Milling of nickel-based superalloy by trochoidal strategies', in 2022 IEEE 22nd International Symposium on Computational Intelligence and Informatics and 8th IEEE International Conference on Recent Achievements in Mechatronics, Automation, Computer Science and Robotics (CINTI-MACRo) 1–6. https://doi.org/10.1109/CINTI-MACRo57952.2022.10029453
40. García-Hernández C et al (2021) 'Trochoidal milling path with variable feed Application to the machining of a Ti-6Al-4V part.' Mathematics 9(21):2701. https://doi.org/10.3390/math9212701
41. Xu K, Wu B, Li Z, Tang K (2019) Time-efficient trochoidal tool path generation for milling arbitrary curved slots. J Manuf Sci Eng 141:3. https://doi.org/10.1115/1.4042052
42. Li Z, Xu K, Tang K (2019) A new trochoidal pattern for slotting operation. Int J Adv Manuf Technol 102:5. https://doi.org/10.1007/s00170-018-2947-0
43. Jacso A, Matyasi G, Szalay T (2019) The fast constant engagement offsetting method for generating milling tool paths. Int J Adv Manuf Technol. https://doi.org/10.1007/s00170-019-03834-8
44. Jacso A, Szalay T (2020) Optimizing the numerical algorithm in fast constant engagement offsetting method for generating 2.5D milling tool paths. Int J Adv Manuf Technol 108:7. https://doi.org/10.1007/s00170-020-05452-1
45. Jacso A, Matyasi G, Szalay T (2020) Trochoidal tool path planning method for slot milling with constant cutter engagement. Lect Notes Mech Eng 8
46. Wu J, Yu G, Gao Y, Wang L (2018) Mechatronics modeling and vibration analysis of a 2-DOF parallel manipulator in a 5-DOF hybrid machine tool. Mech Mach Theory 121:430–445. https://doi.org/10.1016/j.mechmachtheory.2017.10.023
47. Wu J, Wang J, Li T, Wang L (2007) Dynamic analysis of the 2-DOF planar parallel manipulator of a heavy duty hybrid machine tool. Int J Adv Manuf Technol 34(3):413–420. https://doi.org/10.1007/s00170-006-0605-4
48. Póka G, Németh I (2019) The effect of radial rake angle on chip thickness in the case of face milling. Proc Inst Mech Eng Part B J Eng Manuf. https://doi.org/10.1177/0954405419849245

49. Altintas Y (2012) Manufacturing automation: metal cutting mechanics, machine tool vibrations, and CNC design, 2nd Edn. Cambridge University Press
50. Childs T, Maekawa K, Obikawa T, Yamane Y (2000) Metal machining: theory and applications. Elsevier. Available: https://linkinghub.elsevier.com/retrieve/pii/C20090239900. Accessed 1 Jun 2019
51. Guo X et al (2015) Effect of average chip thickness and cutting speed on cutting forces and surface roughness during peripheral up milling of wood flour/polyvinyl chloride composite. Wood Res 60:147–156
52. Jing X, Lv R, Song B, Xu J, Jaffery SHI, Li H (2021) A novel run-out model based on spatial tool position for micro-milling force prediction. J Manuf Process 68:739–749. https://doi.org/10.1016/j.jmapro.2021.06.006
53. Huang J, Du X, Zhu LM (2019) Parallel acceleration/deceleration feedrate scheduling for computer numerical control machine tools based on bi-directional scanning technique. Proc Inst Mech Eng Part B J Eng Manuf 233(3):937–947. https://doi.org/10.1177/0954405417706997
54. Jacso A, Szalay T, Jauregui JC, Resendiz JR (2018) A discrete simulation-based algorithm for the technological investigation of 2.5D milling operations. Proc Inst Mech Eng Part C J Mech Eng Sci: 78–90. https://doi.org/10.1177/0954406218757267.